Borehole seismic modeling with inclusion of tube waves and other tube-wave-related arrivals

Chunling Wu and Jerry M. Harris, Stanford University*

Summary

Borehole seismic data often contain strong tube waves and tube-wave-related arrivals due to the effects of the presence of the borehole. A basic requirement for accurate single-well, cross-well and VSP modeling is inclusion of these events.

We use a velocity-stress variable-grid finite-difference code for cross-well field data modeling with inclusion of the two perforated cased boreholes. The synthetics resemble the field observations in terms of arrival times not only on P- and S-waves but also on tube waves and tube-wave-related arrivals generated by perforations in receiver and source wells.

Introduction

The presence of the borehole has significant effects on borehole seismic surveys. Many of the strongest signals observed are modes traveling within the borehole: these tube waves are often sufficient to cloak the lower amplitude reflections and transmissions. Moreover, tube waves can re-radiate energy into the formation at changes along the borehole to generate tube-wave-related arrivals (White and Lessenger, 1988). A basic requirement for accurate single-well, cross-well and VSP modeling is the inclusion of these events associated with fluid-filled boreholes.

Full-waveform forward modeling is desirable for borehole seismic experiments since not only P-waves but also S-waves are observed in the data. Finite-difference (FD) methods have historically dominated elastic wavefield modeling in geophysics because of their flexibility in representing complex models and their computational efficiency. However, to resolve a small-scale borehole in a reasonable size model by uniform grid FD methods requires too much memory for most computers. Variable-grid FD techniques (Moczo, 1989; Jastram and Behle, 1991; Pitarka, 1999) which allow the use of the fine-grid in the vicinity of boreholes and coarse-grid in the field away from the boreholes overcome the problem and have been applied to borehole seismic modeling (Falk et al., 1996; Wu et al., 2001).

In this paper, a velocity-stress optimized variable-grid FD code (Wu and Harris, 2002) is applied to model a cross-well seismic field data from West Texas with inclusion of the two perforated cased boreholes. Comparison between the synthetic and observed data shows that a good agreement has been achieved not only on direct P and S arrivals, but also on tube waves and tube-wave-related events.

Methods

FD seismic modeling is commonly based on uniform grids. Grid spacing is determined by the smallest length scale present in the model, usually the shortest wavelength. For borehole seismic modeling, the diameter of the borehole is often two or three orders smaller than the shortest seismic wavelength. This forces use of a very fine grid to define the borehole, thus greatly increasing the computational load and restricting calculations to models of very small dimensions. Variable-grid FD techniques provide an efficient solution to this large-scale variation problem.

We use a fourth-order optimized staggered-grid FD operators on a non-uniform mesh for solution of the velocity-stress elastic wave equations (Wu and Harris, 2002). This optimized variable-grid FD scheme has less dispersion errors than the variable-grid FD scheme based on Taylor expansion with the same stencil, thus allowing bigger spacing ratios for grid refinement within transition regions linking fine and coarse-grid domains. We illustrate the model with 2-D examples.

In 2-D, the borehole, casing and perforation are represented as thin layers in x-z plane. The FD gridding scheme is characterized by (1)domains of fine-grid spacing for resolving borehole, casing and perforation, (2)domains of coarse-grid spacing constrained by the shortest wavelength, and (3)transition regions where the grid spacing smoothly varies between these extremes (see Figure 1). The smooth refinement from the coarse-grid spacing to fine-grid spacing avoids the spurious reflection problems associated with sudden changes in grid spacing. The coefficients of the stretched-grid operators are pre-computed. Since the mesh is only distorted along the x and z axis, coefficients are invariant along grid lines, reducing the memory required for stencil storage. The non-uniform mesh is also staggered to increase stability and minimize numerical dispersion: a staggered scheme is crucial for handling the solid-liquid contact present within the borehole. Time derivatives are staggered across the velocity and stress variables and are approximated using an explicit second-order central difference operator.

A parallel version of the algorithm has been developed for more efficient calculations on a "Linux Beowulf" cluster. The parallel implementation utilizes spatial domain decomposition: different portions of the 2-D gridded model are allocated to different processors so that calculations within each such subdomain take place synchronously. Sufficient overlap between adjacent subdo-

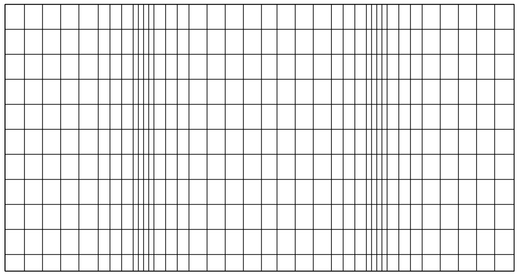

Fig. 1: Non-uniform grid mesh for cross-well models.The horizontal grid spacing is variable to accommodate small-scale boreholes in a large model.

mains/processors must be provided so that the fourth-order spatial FD operators can address all dependent variables at their particular staggered grid storage locations. Inter-processor data communication is based on the MPI (Message Passing Interface).

Field data and modeling study

Field data

The field cross-well data we are analyzing and modeling were collected in the Permian Basin, West Texas. Two cased boreholes with 640 ft separation were used. The source well and receiver well have perforations at the depth of 9000 ft and 8930 ft, respectively.

Figure 2 shows a common-shot gather from this survey. The source is at depth 8695 ft with receiver sampling interval of 5 ft. The depth of the receivers ranges from 8190 to 9200 ft. Note that strong tube waves dominate the wavefields although direct P- and S-waves are clearly seen in some traces. Also tube-wave-related arrivals are observed in the data. These tube-generated body waves are caused by the borehole perforations (Mo and Harris, 1995).

Perforations act as impedance discontinuities in a borehole. In the source well, tube waves will re-radiate energy into the formation at the impedance discontinuities, producing secondary sources. When body waves interact with the receiver borehole, strong tube waves will be generated at the impedance discontinuities. Figure 3 schematically illustrates the wave propagation paths (Figure 3a) and the associated arrivals in the seismogram (Figure 3b) of a common-shot gather. To accurately model this field data requires including borehole, casing and perforation into the modeling scheme.

Modeling study

The 2-D optimized variable-grid FD parallel code is used to model the common shot gather showed in Figure 2 with inclusion of the two perforated cased boreholes. The model is based on the survey geometry. P-wave velocities of the formation are obtained from the blocked V_p log in the source well (Figure 4a). The corresponding S-wave velocities are calculated by $V_s = V_p/\sqrt{3}$. The densities are obtained by $\rho = 0.23{V_p}^{0.25}$ (Gardner et al., 1974). Note in this latter equation, the unit of ρ is g/cm^3 and the unit of V_p is ft/s. Two perforated cased boreholes are embedded in the layered formation. The parameters for the two boreholes are the same: the diameter is 7.2 inch, water-filled, the thickness of the casing and cement is 0.6 inch and 1.2 inch, respectively. Perforations are represented by a small rectangular hole cut through the casing, cement and part of the formation. Figure 1 schematically illustrates the computational mesh used for the model. In the vicinity of the well, the lateral grid spacing smoothly increases from 0.05 ft to 1 ft over a transition region of 1.8 ft wide. The vertical spacing is 1 ft throughout the grid. Spectral analysis reveals that the frequencies in the field data are from 400 Hz to 1200 Hz. We use a Ricker wavelet with 800 Hz central frequency as the source function to excite the model. The calculations were performed on a 16 processor distributed "Linux Beowulf" cluster. One run of 110,000 time steps for a 742*1151 size model takes about 3 hours CPU time.

The synthetic data of the common shot gather is shown in Figure 4b. We see that all the identified arrivals (direct P- and S-waves, strong tube waves and tube-wave related arrivals) in the field data (Figure 2) are observed in the synthetic seismogram. There is a good match between the synthetic and the field observations for these events, especially in terms of the travel times. The difference between the synthetic and the field observations on the amplitude of some events (tube waves generated by direct P- and S-waves, and interface reflections) may due to the attenuation in the real earth.

Conclusions

A 2-D velocity-stress optimized variable-grid FD parallel code has been used for borehole modeling of cross-well field data. Synthetic data not only match the direct P- and S- arrivals in the field observations, but also fit the tube waves and tube-wave-related events generated by the perforations in the source and receiver wells. This study shows that inclusion of borholes into the modeling scheme can distinguish tube-generated events in the data to assist data analysis and to guide field data processing and interpretation.

Future work involves introducing attenuation into modeling to capture amplitude features, and extending to 3-D for more realistic borehole modeling.

Ackonwledgements

Thanks Kaustuv for his help on developing the parallel code.

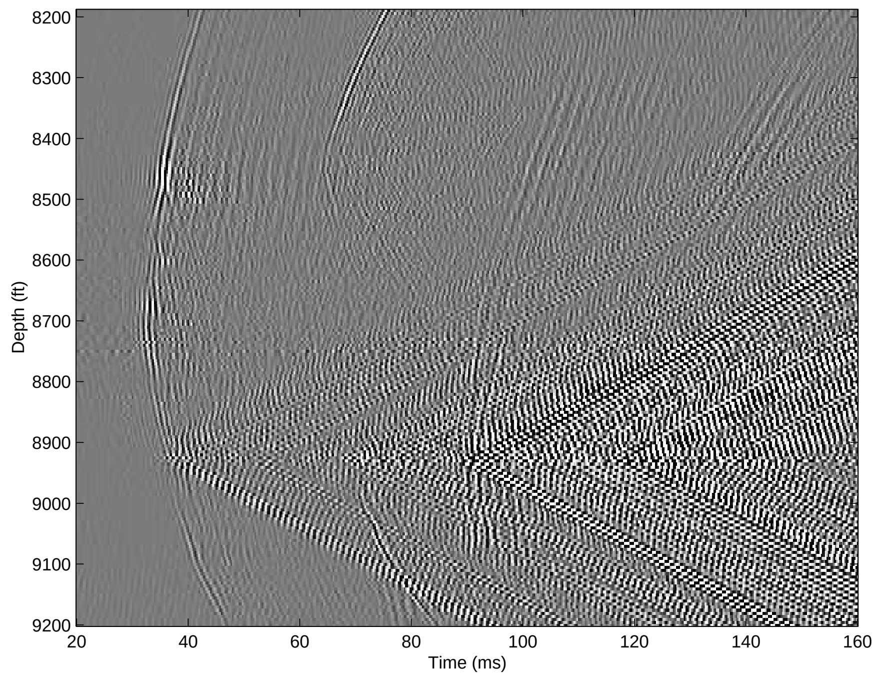

Fig. 2: A common shot gather from the cross-well survey.

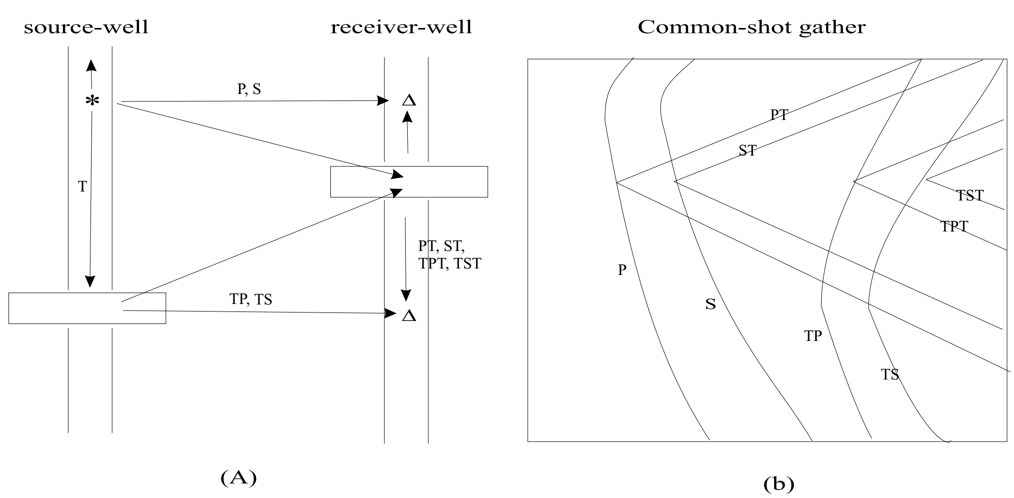

Fig. 3: Schematic diagram of waves in the cross-well survey: (a) Wave paths; (b) Arrivals in the seismogram. P and S are direct P- and S-waves, TP and TS are P and S-waves excited by the secondary source generated by the source tube waves (T) at the perforations in the source well. PT, ST and TPT, TST are receiver tube waves generated by direct body waves and tube-related body waves at the perforations in the receiver well.

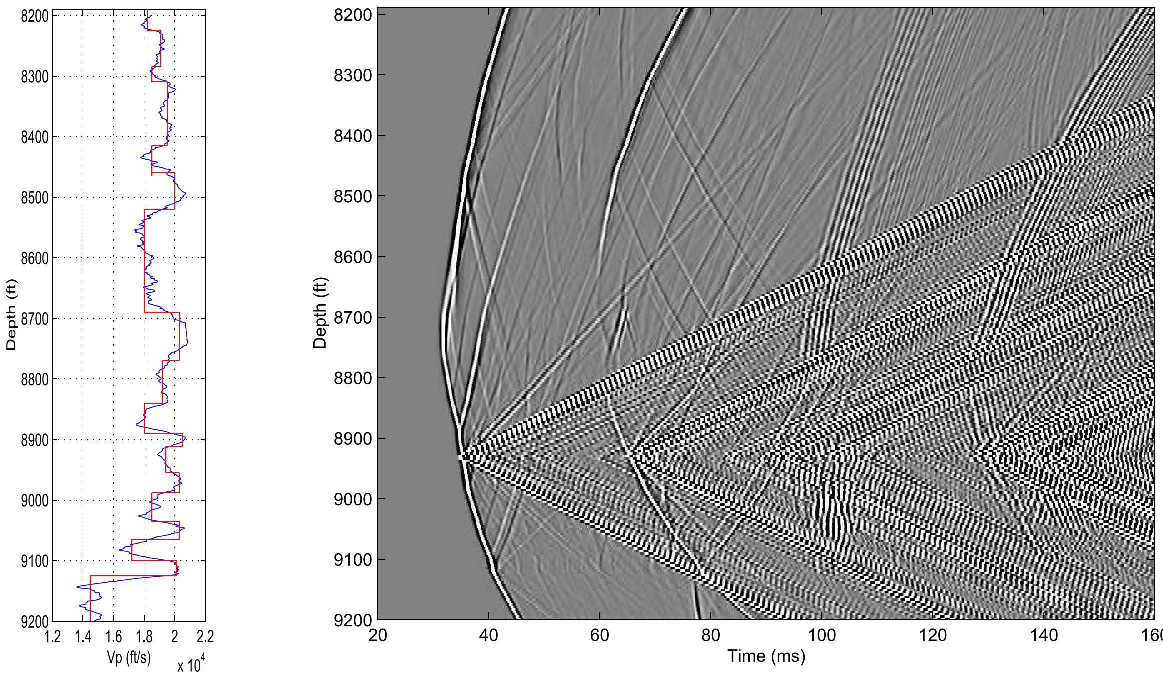

(a) (b)

Fig. 4: (a) Blocked Vp log from the source well; (b) Synthetic seismogram generated by 2-D variable grid FD elastic modeling.

References

Falk, P., Tessmer, E., and D., G., 1996, Tube wave modeling by the finite-difference method with varying grid spacing: PAGEOPH, **148**, 77–92.

Gardner, G. H. F., Gardner, L. W., and Gregory, A. R., 1974, the diagnostic basis for stratigraphic straps: Geophysics, **39**, 770–780.

Jastram, C., and Behle, A., 1991, Elastic modeling by finite-difference and the rapid expansion method (REM): 61st Ann. Internat. Mtg., Soc. Expl. Geophys., 1573–1576.

Mo, L., and Harris, J. M., 1995, Analysis and attenuation of tube waves in crosswell seismic survey: 65th Ann. Internat. Mtg., Soc. Expl. Geophys., 438–441.

Moczo, P., 1989, Finite-difference technique for SH waves in 2-D media using irregular grids-application to the seismic response problem: Geophys. J. int., **99**, 321–329.

Pitarka, A., 1999, 3D elastic finite-difference modeling of seismic motion using staggered grids with nonuniform spacing: Bull. Seism. Soc. Am., **89**, 54–68.

White, J. E., and Lessenger, M. A., 1988, Caliper effect on borehole coupling: Expl. Geophys., **19**, 201–205.

Wu, C., and Harris, J. M., 2002, An optimized variable-grid finite-difference method for seismic forward modeling: SEG Post-Convention Workshop-Advances and limitations in numerical modeling of wave propagation in challenging structures, 72th Ann. Internat. Mtg.

Wu, C., Harris, J. M., and Franklin, J., 2001, Single-well seismic modeling in viscoelastic media using a variable-grid finite-difference method: 71th Ann. Internat. Mtg., Soc. Expl. Geophys., 1155–1158.